Sub-Doppler cooling in reduced-period optical lattice geometries

P. R. Berman, G. Raithel, and R. Zhang
Michigan Center for Theoretical Physics, FOCUS Center, and Physics Department, University of Michigan, Ann Arbor, Michigan 48109-1120, USA

V. S. Malinovsky
MagiQ Technologies, 171 Madison Avenue, Suite 1300, New York, New York 10016, USA
(Received 10 February 2005; revised manuscript received 13 July 2005; published 21 September 2005)

It is shown that sub-Doppler cooling occurs in an atom-field geometry that can lead to reduced-period optical lattices. Four optical fields are combined to produce a "standing wave" Raman field that drives transitions between two ground state sublevels. In contrast to conventional Sisyphus cooling, sub-Doppler cooling to zero velocity occurs when all fields are polarized in the same direction. Solutions are obtained using both semiclassical and quantum Monte Carlo methods in the case of exact two-photon resonance. The connection of the results with conventional Sisyphus cooling is established using a dressed state basis.

DOI: 10.1103/PhysRevA.72.033415 PACS number(s): 32.80.Pj, 32.80.Lg

I. INTRODUCTION

Conventional laser cooling techniques involve the application of counterpropagating laser fields having the same frequency to atoms in a magneto-optical trap. The fields drive transitions between ground and excited electronic state manifolds in the atoms. It is especially important for the ground state manifold to consist of a number of degenerate or nearly degenerate levels to allow for Sisyphus cooling of the atoms [1,2]. Sisyphus cooling can be achieved using cross polarized, counterpropagating laser fields. In this field configuration, the atoms see a spatially modulated polarization gradient that leads to a spatially modulated optical pumping. Sisyphus cooling to zero velocity cannot occur using parallel polarized fields, which produce no spatially varying polarization [3].

The conventional laser cooling schemes have been extended to Raman-type schemes, where *two* sets of standing wave fields drive coupled transitions in a Λ level configuration [4]. Sisyphus cooling can be achieved if the standing wave fields driving the coupled transitions are phase shifted relative to one another, but not if they have the same spatial phase. In both Raman and traditional laser cooling schemes, the basic periodicity of the atomic population distribution is $\lambda/2$, where λ is the laser wavelength. In some cases, the periodicity of *individual* sublevel populations can be $\lambda/4$, but the overall periodicity of the system as a whole remains equal to $\lambda/2$.

Recently, a modified Raman geometry was proposed which reduces this basic periodicity from $\lambda/2$ to $\lambda/4$ [5,6]. The basic geometry is indicated schematically in Fig. 1. Transitions between states $|1\rangle$ and $|2\rangle$ in the Raman scheme occur through the common state $|3\rangle$ using two field modes. Consider first the effect of fields E_1 and E_2. Field E_1, having frequency Ω_1 and wave vector $\mathbf{k}_1=\mathbf{k}=k\hat{\mathbf{z}}$ drives the 1-3 transition while field E_2, having frequency $\Omega_2\approx\Omega_1-\omega_{21}$ and wave vector $\mathbf{k}_2\approx-\mathbf{k}$ drives the 2-3 transition, where ω_{21} is the frequency separation of levels 1 and 2 (it is assumed that $\Omega_2/c\approx\Omega_1/c$, or, equivalently, that $\omega_{21}/\omega_{31}\ll 1$). Owing to polarization selection rules or to the fact that ω_{21} is greater than the detuning $\Delta=\Omega_1-\omega_{31}$, one can neglect any effects related to field E_1 driving the 2-3 transition or field E_2 driving the 1-3 transition [7]. If, in addition, the atom-field detunings on the electronic state transitions are sufficiently large to enable one to adiabatically eliminate state $|3\rangle$, one arrives at an effective two-level system in which states $|1\rangle$ and $|2\rangle$ are coupled by a two-photon "Raman field" having propagation vector $2\mathbf{k}$.

Imagine that we start in state $|1\rangle$. If the initial state $|1\rangle$ amplitude is spatially homogeneous, then, after a two-quantum transition, the final state (state $|2\rangle$) amplitude varies as e^{2ikz}. Such a state amplitude does not correspond to a state $|2\rangle$ population grating, since the final state density is spatially homogeneous. To obtain a density grating one can add *another* pair of counterpropagating fields as shown in Fig. 1. These fields E_3 and E_4 differ in frequency from the initial pair, but the combined two-photon frequencies are equal, $\Omega_1-\Omega_2=\Omega_3-\Omega_4$. The propagation vectors are chosen such

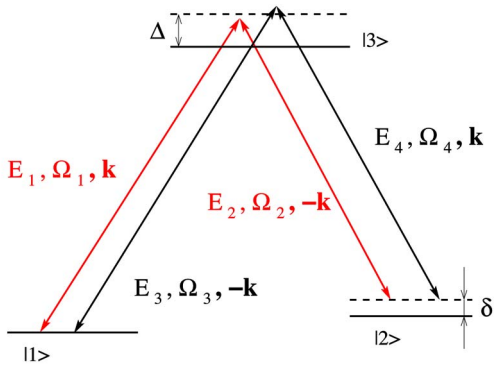

FIG. 1. (Color online) Atom-field geometry that can be used to create a two-photon, standing wave Raman field on the 1-2 transition.

that $\mathbf{k}_3=-\mathbf{k}_4=-\mathbf{k}$. The frequencies of fields E_1 and E_3 are taken to be nearly equal, as are the frequencies of fields E_2 and E_4, but it is assumed that the frequency differences are sufficient to ensure that fields E_1 and E_3 (or E_2 and E_4) do not interfere in driving *single* photon transitions, nor do fields E_1 and E_4 (or E_2 and E_3) drive Raman transitions between levels 1 and 2 [8]. On the other hand, the combined pairs of counterpropagating fields (E_1 and E_2) and (E_3 and E_4) *do* interfere in driving the 1-2 Raman transition and act as a "*standing wave*" Raman field which, to lowest order in the field strengths, leads to a modulation of the final state population given by $\cos(4kz)$. In this manner, a grating having period $\lambda/4$ is created. By using one pair of fields parallel polarized and the other perpendicularly polarized, one can create optical potentials with $\lambda/8$ periodicity [9].

Reduced period optical lattices have potential applications in nanolithography and as efficient scatterers of soft x rays. Moreover, they could be used to increase the density of Bose condensates in a Mott insulator phase when there is exactly one atom per lattice site. With the decreased separation between lattice sites, electric and/or magnetic dipole interactions are increased, allowing one to more easily carry out the entanglement needed in quantum information applications.

Now that it has been established that this *standing-wave Raman scheme* (SWRS) leads to optical lattices having reduced periodicity, the question arises naturally whether or not some type of sub-Doppler or Sisyphus cooling is present in this scheme. A sub-Doppler cooling mechanism would simplify the experimental realization of this new type of optical lattice. It is by no means obvious that Sisyphus cooling occurs in this SWRS. In this paper, laser cooling in the SWRS is examined in detail for two-photon resonance of the Raman fields, $\delta=\Omega_1-\Omega_2-\omega_{21}=\Omega_3-\Omega_4-\omega_{21}=0$. The friction force and diffusion coefficients are calculated using a semiclassical approach and are shown to be very similar to those obtained in standard Sisyphus cooling. A dressed atom picture is introduced to help facilitate the comparison of the SWRS with conventional Sisyphus cooling. The calculation is repeated using a quantum Monte Carlo approach [10] and the results are compared with those of the semiclassical model. In a future planned publication, the calculations are extended to allow for nonresonant Raman detunings, $\delta\neq 0$. Subsequent to the submission of this paper, an experiment has been carried out that provides the first evidence for this SWRS sub-Doppler cooling [11].

II. PHYSICAL ORIGIN OF THE FRICTION FORCE

To understand the physical origin of the friction force for our atom-field geometry, it is useful to review the mechanisms responsible for sub-Doppler cooling. In polarization gradient cooling of a $J=1/2$ ground state, a Sisyphus picture of cooling has proven useful [1]. In this picture there are potential curves for each ground state sublevel; an atom climbs a hill of one potential and is transferred to a trough of the other potential via spontaneous emission. There is, however, an alternative picture of the cooling [12]. The incident counter-propagating fields create a matter wave grating for the population difference of the two ground state sublevels and scatter off this grating. As a result, momentum is exchanged between the fields *provided* that there is a nonvanishing phase shift between the field and matter wave gratings. It is easy to show that such a phase shift exists only in the presence of dissipation (spontaneous emission) and only for atoms having nonzero velocity. The momentum exchange between the fields is responsible for the friction force [12].

Since we are not dealing with polarization gradient cooling in our atom field geometry, we must consider two additional mechanisms responsible for sub-Doppler cooling. Both mechanisms arise for the atom-field geometry of Fig. 1. The first of these has been discussed by Dalibard and Cohen-Tannoudji in the context of "corkscrew" cooling using σ_+ and σ_- counterpropagating fields for a $J=1$ ground state and a single pair of Raman fields [1]. These fields do not result in a spatially modulated population of the ground state sublevels, but they do give rise to an imbalance in the populations of the ground state sublevels if the effective detuning, $\tilde{\delta}=\delta-2kv$ is not equal to zero (v is the z component of atomic velocity). As a result of the imbalance, the scattering rate for each of the incident fields differs and the difference results in a friction force on the atoms. There is an additional mechanism present in the corkscrew polarization scheme [1,13]. The incident fields lead to a spatially modulated phase coherence between ground state sublevels (in this paper, the term "coherence" refers to nonvanishing off-diagonal density matrix elements). In analogy with the case of a driven oscillator, it is possible for the incident fields to exchange momentum if the matter wave phase coherence is out of phase with the phase coherence of the fields. This will occur only in the presence of dissipation (spontaneous emission) and only for atoms having $\tilde{\delta}\neq 0$. For the $J=1$ to $J=2$ transition considered by Dalibard and Cohen-Tannoudji [1], the major contribution to the friction force comes from the imbalance in the sublevel populations.

We are now ready to address the origin of the friction force in our atom field geometry. Mathematical justification for this qualitative discussion is given in Appendix B. Consider first the action of a single pair of Raman field (e.g., fields E_1 and E_2). It is known that the friction force *vanishes* in this case, provided the branching ratios for decay of level 3 to each of levels 1 and 2 are equal (as is assumed) [13–15]. The vanishing of the friction force can be understood in terms of an *exact cancellation* of the contribution associated with an imbalance of population of levels 1 and 2 by the contribution associated with the spatially modulated phase coherence of ρ_{12} induced by the fields [13]. When the *second* pair of Raman fields (E_3 and E_4) is added, the contributions from the population imbalance *cancel*, regardless of the detuning, provided that the Rabi frequencies associated with all the atom-field transitions are equal. In this limit, the spatially averaged friction force results solely from momentum exchange between the fields that is mediated by the spatially modulated phase coherence $\rho_{12}\sim e^{\pm 2ikz}$. Of course, this contribution is nonvanishing only in the presence of dissipation.

From this qualitative discussion, it should be apparent that the underlying physical mechanism responsible for sub-Doppler cooling in our atom-field geometry differs from that of conventional sub-Doppler cooling. An alternative explanation of the cooling mechanism can be given in terms of dressed states (see Sec. V); in that case one recovers the conventional explanation in terms of Sisyphus cooling.

III. SEMICLASSICAL TREATMENT

The basic physics is illustrated if we consider the somewhat unphysical level scheme in which states $|1\rangle$ and $|2\rangle$ in Fig. 1 have angular momentum $J=0$, while the upper level has angular momentum $J=1$ [16]. The fields all are assumed to be linearly polarized in the x direction; there is no polarization gradient. The fields couple the ground state to the excited state $|3\rangle=(|J=1,m=-1\rangle-|J=1,m=1\rangle)/\sqrt{2}$. The field intensities are adjusted such that the Rabi frequencies χ (assumed real) associated with all the atom-field transitions are equal (Rabi frequencies are defined by $-\mu E/2\hbar$, where μ is the x component of the dipole moment matrix element between ground and excited states), and the partial decay rate of level 3 to each of levels 1 and 2 is taken equal to $\Gamma/2$ (equal branching ratios for the two transitions). The results would be unchanged if the fields were all σ_+ polarized.

In the rotating-wave approximation and neglecting spontaneous emission, the Hamiltonian for the atom-field system is

$$H=\sum_{j=1}^{3}\hbar\omega_j|j\rangle\langle j+\hbar\chi[|1\rangle\langle 3|(e^{-i(kz-\Omega_1 t)}+e^{-i(-kz-\Omega_3 t)}) + |2\rangle\langle 3|(e^{-i(-kz-\Omega_2 t)}+e^{-i(kz-\Omega_4 t)})+\text{adj}], \tag{1}$$

where $\hbar\omega_j$ is the energy of level j and "adj" stands for adjoint. It is assumed that the electronic state detunings are sufficiently large to satisfy

$$\Omega_1-\omega_{31}\approx\Omega_3-\omega_{31}\approx\Omega_2-\omega_{32}\approx\Omega_4-\omega_{32}\equiv\Delta\gg\Gamma,\chi,kv.$$

In this limit and in the rotating-wave approximation, it is possible to adiabatically eliminate state $|3\rangle$ and to obtain equations of motion for density matrix elements [17,18]. For classical center-of-mass motion ($d\rho_{ij}/dt=\partial\rho_{ij}/\partial t+v\partial\rho_{ij}/\partial z$), using a field interaction representation [19], and including spontaneous emission [20], one finds the *steady-state* equations of motion for density matrix elements to be

$$\alpha\frac{\partial w}{\partial x}=-w+2i\sigma(\rho_{21}-\rho_{12})\cos x,$$

$$\alpha\frac{\partial\rho_{12}}{\partial x}=-(1+id)\rho_{12}-i\sigma w\cos x-\frac{1}{2}\cos x, \tag{2}$$

where $w=\rho_{22}-\rho_{11}$ is the population difference of levels 2 and 1,

$$\delta=\Omega_1-\Omega_2-\omega_{21}=\Omega_3-\Omega_4-\omega_{21} \tag{3}$$

is the Raman detuning,

$$x=2kz, \tag{4a}$$

$$d=\frac{\delta}{2\Gamma'}, \tag{4b}$$

$$\alpha=kv/\Gamma', \tag{4c}$$

$$\sigma=\Delta/\Gamma, \tag{4d}$$

$$\Gamma'=\Gamma\chi^2/[\Delta^2+(\Gamma/2)^2]\sim\chi^2\Gamma/\Delta^2 \tag{4e}$$

is an optical pumping rate, and v is the z component of atomic velocity. As noted above, interference between fields E_1 and E_3 (or E_2 and E_4) in driving *single* photon transitions is neglected in deriving these equations, as is the combined action of fields E_1 and E_4 (or E_2 and E_3) in driving Raman transitions between states $|1\rangle$ and $|2\rangle$. Equations (2) reflect the combined effects of the Raman fields driving transitions between levels 1 and 2 and the loss of coherence resulting from spontaneous emission.

For $d\neq 0$, Eqs. (2) must be solved numerically; however, as is seen below, an analytical solution can be obtained if $d=0$. Note that there is now a source term, $-\frac{1}{2}\cos x$, in the equation for ρ_{12} that can be traced to the fact that the factor $(\rho_{11}+\rho_{22})$ that multiplies this term is equal to unity. Steady state is reached on a time scale $\Gamma'^{-1}\gg\Gamma^{-1}$. The atom-field "coupling strength" σ is actually independent of field strength in these dimensionless units. Note that, for zero velocity atoms, $\alpha=0$, and for zero detuning $d=0$, the population difference w vanishes, while the coherence $\rho_{12}=-\frac{1}{2}\cos x$ is spatially modulated. This is in contrast to conventional Sisyphus cooling, where the coherence vanishes while the population difference is spatially modulated.

In Appendix A, Eqs. (2) are modified to include diffusion resulting from changes in atomic momentum associated with stimulated emission and absorption, as well as spontaneous emission. The total population $S=\rho_{11}+\rho_{22}$ now becomes a function of momentum and position, although the dependence of S on position is neglected [21,22]. The modified equations are

$$\alpha\frac{\partial}{\partial x}\begin{pmatrix}u\\g\\w\end{pmatrix}=\begin{pmatrix}-1 & d & 0\\ -d & -1 & -2\sigma\cos x\\ 0 & 2\sigma\cos x & -1\end{pmatrix}\begin{pmatrix}u\\g\\w\end{pmatrix}-\begin{pmatrix}\cos xS+2\sigma\hbar k\sin x\dfrac{\partial S}{\partial p}\\ 0\\ 0\end{pmatrix}, \tag{5a}$$

$$\frac{\partial S}{\partial t}=\frac{7}{5}\hbar^2k^2\Gamma'\frac{\partial^2 S}{\partial p^2}-4\Gamma'\sigma\hbar k\sin x\frac{\partial u}{\partial p}-\frac{3}{5}\hbar^2k^2\Gamma'\cos x\frac{\partial^2 u}{\partial p^2}, \tag{5b}$$

where $u=\rho_{12}+\rho_{21}$ and $g=i(\rho_{21}-\rho_{12})$. Each of the functions u,g,w are now functions of the momentum $p=Mv$ (M is the atom's mass) as well as x. Equation (5a) is solved for u,g,w and the solution for u is inserted into Eq. (5b) for S. The resultant equation is averaged over a wavelength such that

$$\frac{\partial S}{\partial t} = \frac{7}{5}\hbar^2 k^2 \Gamma' \frac{\partial^2 S}{\partial p^2} - 4\Gamma' \sigma \hbar k \overline{\sin x \frac{\partial u}{\partial p}} - \frac{3}{5}\hbar^2 k^2 \Gamma' \overline{\cos x \frac{\partial^2 u}{\partial p^2}}, \tag{6}$$

where the bar indicates a spatial average ($\bar{S}=S$, by assumption). In this paper, only the limit of zero Raman detuning, $d=0$, is considered.

If $d=0$, the equation for u is decoupled from the others and both g and w vanish owing to the lack of any source term. The appropriate solution for u, periodic in the variable x, is given by

$$\begin{aligned} u &= -\frac{1}{\alpha}\int_{-\infty}^{x} dx' e^{-(x-x')/\alpha}\left(\cos x' S + 2\sigma\hbar k \sin x' \frac{\partial S}{\partial p}\right) \\ &= -\frac{1}{1+\alpha^2}\left\{ S(\cos x + \alpha \sin x) \right. \\ &\quad \left. + 2\sigma\hbar k \frac{\partial S}{\partial p}(\sin x - \alpha \cos x)\right\}. \end{aligned} \tag{7}$$

When this solution is substituted into Eq. (5b) and the resulting equation is compared with the Fokker-Planck equation

$$\frac{\partial S}{\partial t} = \frac{\partial}{\partial p}\left[-\bar{F}S + \bar{D}_{ind}\frac{\partial S}{\partial p} + \frac{\partial}{\partial p}[\bar{D}_{sp}S]\right], \tag{8}$$

one can identify the spatially averaged friction force

$$\bar{F} = -2\Gamma' \sigma \hbar k \frac{\alpha}{1+\alpha^2}, \tag{9}$$

and the spatially averaged diffusion coefficients

$$\bar{D}_{sp} = \hbar^2 k^2 \Gamma' \left(\frac{7}{5} + \frac{3}{10}\frac{1}{1+\alpha^2}\right), \tag{10}$$

$$\bar{D}_{ind} = 4\Gamma' \sigma^2 \hbar^2 k^2 \frac{1}{1+\alpha^2}, \tag{11}$$

where $\alpha=kp/M\Gamma'$. These results are very similar to those found in conventional Sisyphus cooling [21,22].

Energy distribution

The steady state solution of the Fokker-Planck equation, subject to the boundary condition $\partial S/\partial p)_{p=0}=0$, is given by

$$S(p) = S(0)\exp\left[\int_0^p dp' \frac{\left(\bar{F} - \frac{\partial \bar{D}_{sp}}{\partial p'}\right)}{\bar{D}_{ind} + \bar{D}_{sp}}\right]. \tag{12}$$

Since $\alpha=kv/\Gamma'=kp/M\Gamma'$, one has

$$\frac{\partial \bar{D}_{sp}}{\partial p} = -\frac{6}{5}\hbar k \omega_r \frac{\alpha}{(1+\alpha^2)^2}, \tag{13}$$

where

$$\omega_r = \frac{\hbar k^2}{2M} \tag{14}$$

is the recoil frequency associated with a one-photon transition. Defining $\alpha'=kp'/M\Gamma'$, one finds that the integral in Eq. (12) can be recast in the form

$$\int_0^p dp' \frac{\left(\bar{F} - \frac{\partial \bar{D}_{sp}}{\partial p'}\right)}{\bar{D}_{ind} + \bar{D}_{sp}} = \int_0^\alpha d\alpha' \frac{\alpha'}{1+\alpha'^2} \frac{\frac{3}{5} - I'(1+\alpha'^2)}{4\sigma^2 + \frac{7}{5}(1+\alpha'^2) + \frac{3}{10}}, \tag{15}$$

where

$$I' = I\frac{4\sigma^2}{1+4\sigma^2}, \quad I = \chi^2/(\Delta\omega_r).$$

It then follows from Eqs. (12) and (15) that

$$S(\bar{p}) = S(0)\left(1+\frac{\bar{p}^2}{\bar{p}_c^2}\right)^{\beta_0} \frac{1}{\left(1+\frac{\bar{p}^2}{\bar{p}_c^2}\beta_1\right)^{\xi+\beta_0}}, \tag{16}$$

where

$$\bar{p} = p/\hbar k, \quad \bar{p}_c = \frac{\Gamma'}{2\omega_r},$$

$$\beta_0 = \frac{1}{1+\frac{40}{3}\sigma^2} \approx 0, \tag{17a}$$

$$\beta_1 = \frac{14}{40\sigma^2+17} \approx \frac{7\Gamma^2}{20\Delta^2}, \tag{17b}$$

$$\xi = \frac{5}{14} I \frac{1}{1+\frac{1}{4\sigma^2}} \approx \frac{5}{14} I. \tag{17c}$$

The momentum distribution $S(\bar{p})$ depends on two parameters, $\sigma=\Delta/\Gamma$ and the dimensionless Raman intensity $I=\chi^2/(\Delta\omega_r)$.

The mean equilibrium kinetic energy can be calculated as

$$E_{eq} = E_r \frac{\int_{-\infty}^{\infty} \bar{p}^2 S(\bar{p}) d\bar{p}}{\int_{-\infty}^{\infty} S(\bar{p}) d\bar{p}},$$

where $E_r=\hbar\omega_r$ is the recoil energy. The integrals can be evaluated analytically and, for $I>21/5$, one finds

$$E_{eq}/E_r = \bar{p}_c^2 \left[\frac{\sqrt{\pi}}{2} \Gamma\left[-\frac{3}{2}-\beta_0\right] \Gamma[\beta_0+\xi]\, {}_2F_1\left[\frac{3}{2}, \xi+\beta_0, \frac{5}{2}+\beta_0, \beta_1\right] + \frac{\Gamma\left[-\frac{3}{2}+\xi\right]\Gamma\left[\frac{3}{2}+\beta_0\right]\Gamma[-\beta_0]}{\beta_1^{3/2+\beta_0}} {}_2F_1\left[-\frac{3}{2}+\xi, -\beta_0, -\frac{1}{2}-\beta_0, \xi\right] \right] \left[\sqrt{\pi}\Gamma\left[-\frac{1}{2}-\beta_0\right]\Gamma[\beta_0+\xi]\, {}_2F_1\left[\frac{1}{2}, \xi+\beta_0, \frac{3}{2}+\beta_0, \beta_1\right] + \frac{\Gamma\left[-\frac{1}{2}+\xi\right]\Gamma\left[\frac{1}{2}+\beta_0\right]\Gamma[-\beta_0]}{\beta_1^{1/2+\beta_0}} {}_2F_1\left[-\frac{1}{2}+\xi, -\beta_0, \frac{1}{2}-\beta_0, \xi\right] \right]^{-1}, \tag{18}$$

where $\Gamma[\cdots]$ is the Euler gamma function (not to be confused with the decay rate Γ) and ${}_2F_1$ is a hypergeometric function. With the approximations $\beta_0 \approx 0$, $\beta_1 \approx 7\Gamma^2/20\Delta^2$, $\xi \approx \frac{5}{14} I$, this reduces to

$$\frac{E_{eq}}{E_r} = \frac{I^2}{I - \frac{21}{5}}. \tag{19}$$

The momentum distribution $S(\bar{p})$, given by Eq. (16), is shown in Fig. 2 as a function of scaled intensity I. Maximum cooling, which corresponds to the narrowest momentum distribution, is obtained for $I \approx 8.4$ in good agreement with Eq. (19). More details about the form of the momentum distribution and mean equilibrium kinetic energy are provided in the next section.

IV. QUANTUM MONTE CARLO APPROACH

To gain further insight into the cooling dynamics, we solve the problem using quantum Monte Carlo wave function simulations (QMCWF) [10,23]. The simulations employ a fully quantum-mechanical description of the center-of-mass motion and allow us to determine the spatial and momentum distributions of the atoms, including the degree to which the atoms become localized in the wells of the Raman optical-lattice potentials. Also, the dynamics of the cooling process can be studied in detail.

In the QMCWF method, the evolution of the density matrix describing the atoms in the lattice is obtained by forming averages over N quantum trajectories $|\psi_i(t)\rangle$, each of which is a realization of a single-atom wave function evolution:

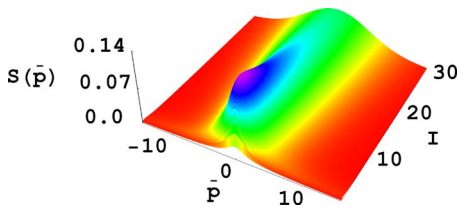

FIG. 2. (Color online) Momentum distribution, $S(\bar{p})$, as a function of $I = \chi^2/(\Delta\omega_r)$ for $\sigma = \Delta/\Gamma = 10$.

$$\rho(t) = \sum_{i=1}^{N} \frac{1}{N} \frac{|\psi_i(t)\rangle\langle\psi_i(t)|}{\langle\psi_i(t)||\psi_i(t)\rangle}. \tag{20}$$

Averages are taken over ensembles of typically $N = 10^4$ to $N = 10^5$ quantum trajectories.

Each quantum trajectory contains periods of deterministic Hamiltonian wave function evolution, connected by discrete quantum jumps. The Hamiltonian evolution is governed by an effective Hamiltonian $H = H_{\rm kin} + H_{\rm pot}$ with a kinetic part $H_{\rm kin} = \hat{p}^2/2M$ and a potential operator $H_{\rm pot}$. The latter describes the coherent interaction between atoms and light fields, and wave function damping caused by photon scattering [10]. As in the semiclassical treatment, in our QMCWF the excited-state components of the wave functions are adiabatically eliminated. Consequently, matrix elements of the potential operator are of the form

$$\langle z', m'|H_{\rm pot}|z, m\rangle = \frac{\hbar\chi^2}{\Delta + i\Gamma/2} A_{m',m}(z)\,\delta(z'-z) \tag{21}$$

with an internal-state quantum number $m \in \{1, 2\}$ denoting the two ground states. The imaginary part in the energy denominator leads to a gradual decay of the wave function norm. The elements $A_{m',m}(z)$, written in a conventional interaction representation, are given by

$$A_{1,1}(z,t) = 2[1 + \cos(2kz - \delta_u t + \phi_{13})],$$

$$A_{2,2}(z,t) = 2[1 + \cos(2kz + \delta_u t + \phi_{42})],$$

$$A_{1,2}(z,t) = 2e^{i\theta/2} e^{i\delta t} \cos(2kz - \phi/2) + e^{i[(\delta+\delta_u)t+\phi_{41}]} + e^{i[(\delta-\delta_u)t+\phi_{23}]},$$

$$A_{2,1}(z,t) = A_{1,2}^*(z,t), \tag{22}$$

where $\delta_u = \Omega_1 - \Omega_3 = \Omega_2 - \Omega_4$, $\phi_{ij} = \phi_i - \phi_j$, $\phi = \phi_{21} - \phi_{43}$, $\theta = \phi_{21} + \phi_{43}$, and the ϕ_i are the phases of the individual fields. The terms $A_{1,1}(z,t)$ and $A_{2,2}(z,t)$ are proportional to the ac stark shift of levels 1 and 2. There is a common shift of both levels that can be ignored and a moving spatial grating that contributes negligibly, owing to the fact that $|\delta_u| \gg \Gamma'$. The second two terms in the transition matrix element $A_{1,2}(z,t)$ also average to zero on the assumption that $|\delta_u| \gg \Gamma', |\delta|$; the

remaining term in $A_{1,2}(z,t)$ contains a spatial lattice phase shift ϕ and a phase factor $e^{i\theta/2}$. The spatial phase shift corresponds to a global shift of the lattice and can be ignored. The phase θ is unimportant if spontaneous emission does not result in the creation of coherence between states $|1\rangle$ and $|2\rangle$. In this work, any such contributions are neglected, owing to the assumption that the frequency separation of levels 1 and 2 is much larger than Γ' [24].

The quantum trajectories are represented in a basis $\{|p_n=\hbar(2nk_L+q),m\rangle\}$, where $k_L=2\pi/\lambda$, n is an integer with $-n_{\max}\leqslant n\leqslant n_{\max}$ and $n_{\max}=16$ or 32. The continuous momentum variable $\hbar q$, which satisfies $-k_L<q<k_L$ and is associated with recoil on spontaneous emission, does not change during the Hamiltonian portions of the wave function evolution, as can be seen by inspection of the matrix elements of $A(z)$. The Hamiltonian evolution is carried out numerically in discrete time steps. We use a split-operator method [25], in which the kinetic-energy operator, which is diagonal in the momentum basis, is applied in the momentum basis, while the atom-field interaction, which is diagonal in position, is applied in a position basis. Thus, at each time step the quantum trajectory is transformed back and forth between position and momentum representations using FFT's. Consequently, both the position and the momentum probability distributions of the quantum trajectory $|\psi\rangle$ can be obtained without numerical overhead at any time of the quantum trajectory evolution.

The periods of Hamiltonian evolution are interrupted by discrete quantum jumps, which simulate the effect of the spontaneous scattering of lattice photons. The time instants and effects of the quantum jumps are governed by quantum-mechanical probability laws [10]. In each quantum jump, random numbers are drawn to select the type of transition—into state $|1\rangle$ or state $|2\rangle$—and the direction of the spontaneously emitted photon. The applied radiation pattern is that of a linearly polarized dipole aligned perpendicular to the direction of the lattice beams. In each jump, the wave function is modified in a well-defined manner, unambiguously determined by the wave function prior to the jump and by the rules of quantum measurement of a spontaneous photon of the selected type.

We study first the dependence of steady-state kinetic energy on the dimensionless Raman intensity $I=\chi^2/\Delta\omega_r$. Steady-state energies are displayed in Fig. 3 for $\sigma=\Delta/\Gamma=2,16$. In the figure, the simulation results are compared with those obtained from the semiclassical theory. In both the QMCWF and the semiclassical calculations, in the range $I\gtrsim 10$ the energy scales linearly with I. The energy values obtained in the QMCWF are about 30% lower than those obtained in the semiclassical calculations. This systematic difference is attributed to the beneficial effect of atomic localization in the lattice wells, which is accounted for in the QMCWF, but not in the semiclassical theory. A similar behavior has been observed earlier for Sisyphus cooling in conventional optical lattices [21].

The QMCWF results in Fig. 3 show that the energy reaches a minimum $E_{\min}\approx 12E_r$ at $I\approx 10$, compared with the results of the semiclassical model, in which $E_{\min}=16.8E_r$ at $I=8.4$. At lower values of I the energy quickly diverges, and the uncertainties in the QMCWF become substantial. The

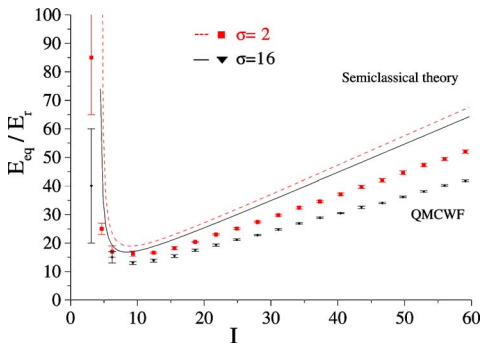

FIG. 3. (Color online) Dimensionless steady-state kinetic energy obtained using QMCWF simulations (symbols with error bars) and semiclassical calculations (lines) as a function of dimensionless intensity $I=\chi^2/\Delta\omega_r$ for $\sigma=2,16$.

increase in uncertainty of the QMCWF results in the range $I<10$ is due to the fact that in this range the cooling dynamics becomes very slow. Thus, it becomes questionable in the QMCWF whether or not steady state is reached. The issue is amplified by the fact that for $I<10$ the atoms undergo so-called Levy flights, as in standard Sisyphus cooling [26]. The Levy flights are phases in which the atoms have abnormally large kinetic energies. The Levy flights are quite rare events and interrupt much longer phases in which the atoms are cooled to very low kinetic energy. Owing to these properties of the Levy flights, in QMCWF it is problematic to achieve small statistical errors of the kinetic energy in the range $I<10$. It is noteworthy that in the range $I\gtrsim 10$ the Levy flights quickly disappear. Therefore, the uncertainties of QMCWF results drop rapidly for $I\gtrsim 10$.

Figure 4 shows several examples of the momentum distribution obtained using the QMCWF and semiclassical models. It is seen that the momentum distribution changes dramatically as a function of scaled intensity I. We have examined QMCWF and semiclassical momentum distributions for a wide range of intensities and found that the distributions varied from being close to Gaussian for $I\gg 10$ to

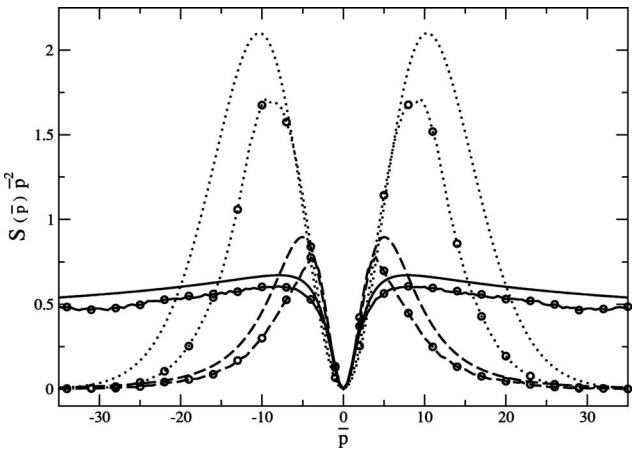

FIG. 4. Graphs of the momentum distribution, $S(\bar{p})$, multiplied by $\bar{p}^2$ for $\sigma=8$ and several values of I: $I=3.11$, solid line; $I=8.4$, dashed line; $I=50$, dotted line; lines, semiclassical theory; lines with circles, QMCWF.

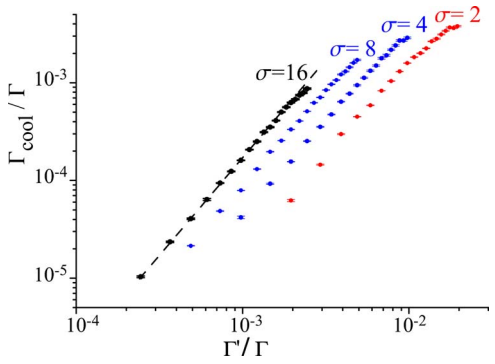

FIG. 5. (Color online) Dimensionless cooling rate vs Γ'/Γ for several values of σ. The dashed line shows a quadratic fit to the data for $\sigma=16$.

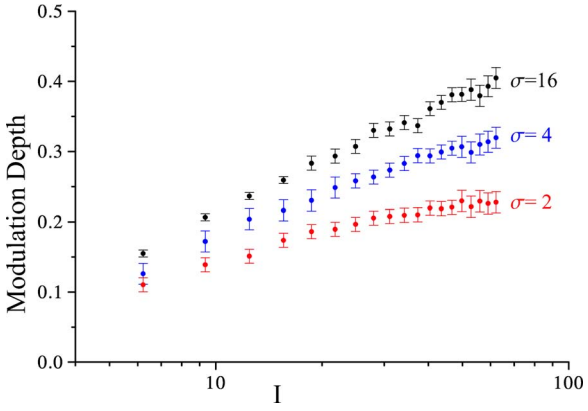

FIG. 6. (Color online) Modulation depth of the density distribution of the atoms in the lattice wells vs I for several values of σ.

nearly Lorentzian for $I\sim 10$. It can also be seen in the figure that the QMCWF simulations lead to momentum distributions that are narrower than the semiclassical ones. This effect can be attributed to localization in the lattice wells and results in lower mean equilibrium kinetic energies (Fig. 3).

In the range of robust cooling, $I\gtrsim 10$, the time dependence of the kinetic energy is found to be of the form $E_{kin}(t)=E_0+E_1e^{-\Gamma_{cool}t}$. The constants E_0 and E_1 and the cooling rate Γ_{cool} depend on lattice and atomic parameters. In Fig. 5 we show cooling rates obtained for typical Raman lattices. It is noted that the cooling rates saturate at a Δ-dependent value and can be as large as $0.2\Gamma'$ (see data for $\sigma=2$). Also, considering fits of the cooling rates such as the one displayed for $\sigma=16$, it is seen that the cooling rate tends to be a quadratic function of the photon scattering rate Γ'. In conventional Sisyphus cooling the cooling rate tends to be more a linear function of the photon scattering rate [27].

For $I<10$ the energy $E_{kin}(t)$ cannot be represented by a simple analytical approximation. In this range, $E_{kin}(t)$ initially decays exponentially (to a good approximation), followed by a much slower cooling to steady state. The presence of multiple time scales in the cooling process apparently reflects a shrinking velocity capture range of the cooling process for $I<10$. At such low lattice intensities, atoms with initial velocities within the capture range are cooled quickly, while atoms with larger velocities are cooled much more slowly. Further study will be required to entirely understand the cooling dynamics.

The QMCWF also yield data on the modulation depth of the density distribution of the atoms in the lattice wells. The spatial density distribution generally is found to have a periodicity of $\lambda/4$, in agreement with the discussion in Sec. I. Quantitatively, we find that the modulation depth of the density distribution increases with I and Δ, as seen in Fig. 6. It is concluded that it is fairly easy to achieve a relative modulation amplitude of order 0.4 (the relative modulation amplitude is defined as the difference between maximum and minimum density divided by their sum).

V. DRESSED STATES

The fact that one recovers the results of Sisyphus cooling for $\delta=0$ suggests that there is a representation where the Sisyphus picture emerges naturally. One might think that the appropriate basis is a semiclassical dressed state basis in which one diagonalizes the Hamiltonian

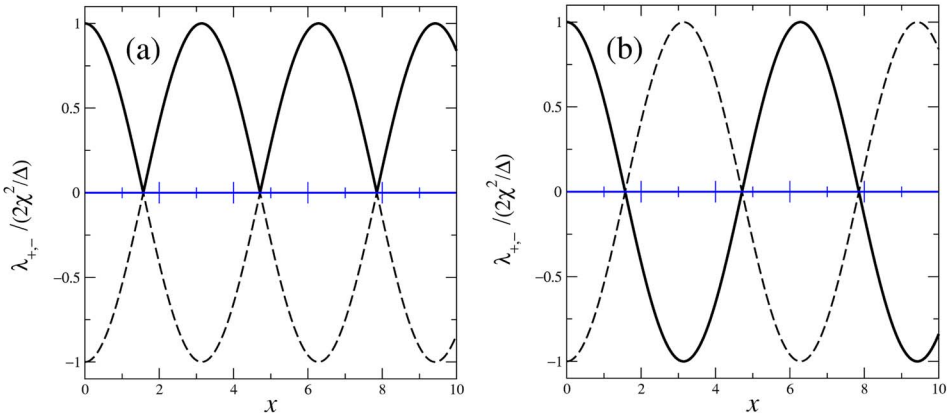

FIG. 7. (Color online) Graphs of the dressed-state optical potentials (a) and the modified dressed state potentials (b). Solid line, λ_+; dashed line, λ_-.

$$H = \frac{\hbar}{2}\begin{pmatrix} \delta & \frac{4\chi^2}{\Delta}\cos x \\ \frac{4\chi^2}{\Delta}\cos x & -\delta \end{pmatrix}.$$

When $\delta=0$, the eigenvalues of H are given by

$$\lambda_{\pm} = \pm\left|\frac{2\chi^2}{\Delta}\cos x\right|.$$

The potentials are drawn in Fig. 7(a) as a function of x. Since each eigenvalue is either always positive or always negative, these potentials are not those associated with Sisyphus cooling. Moreover, nonadiabatic coupling occurs whenever the potentials meet. Instead of using conventional dressed states, one could use modified dressed states in which the eigenvalues are $\lambda_{\pm}\sim\pm 2(\chi^2/\Delta)\cos x$. The corresponding potentials shown in Fig. 7(b) are totally equivalent to the conventional Sisyphus potentials. The dressed eigenstates are analogous to the bare states of conventional Sisyphus cooling. As such, for zero velocity atoms, the dressed state coherence vanishes, while the dressed state population difference is spatially modulated; in other words, populations and coherences are interchanged in going from the bare to dressed basis. The interpretation in terms of these modified dressed states is useful only for $\delta=0$; for $\delta\neq 0$, one must revert to conventional dressed states, and nonadiabatic coupling near the potential extrema can play a role. This will be explored in a future paper.

VI. SUMMARY

We have shown that sub-Doppler cooling occurs for a standing-wave Raman scheme (SWRS) that results in reduced period optical lattices. Both semiclassical and quantum Monte Carlo calculations were carried out for the case of exact two-photon resonance. The results from the two approaches were in qualitative agreement, but the role of spatial localization leads to effects that are not included in the simplified semiclassical method. It was possible to draw an analogy with conventional Sisyphus cooling if a transformation to a new basis was made. In a future planned paper, the calculations will be extended to nonzero Raman detunings.

It is relatively straightforward to generalize these results to situations in which optical lattices having periodicity $\lambda/2n$ can be produced (n is a positive integer greater than 1) [5,28,29]. If the Raman detuning δ is chosen equal to $-\omega_{21}/n$, then it will take n two-photon processes to achieve resonance between states $|1\rangle$ and $|2\rangle$. If $\omega_{21}/n\gg\Gamma'$, the 1-2 transition is, in effect, driven by a $2n$-photon process and the resultant overall periodicity is reduced to $\lambda/2n$.

ACKNOWLEDGMENTS

This research is supported by National Science Foundation under Grants No. PHY-0244841, PHY-0245522, and the FOCUS Center Grant, and by the U. S. Army Research Office under Grant No. DAAD19-00-1-0412.

APPENDIX A

The starting point for the derivation of the Fokker-Planck equation is Eq. (4.10) of Ref. [30]. This equation is written in momentum space for quantized center-of-mass states and includes effects related to changes in atomic momentum resulting from both stimulated and spontaneous emission. Equation (4.10) of Ref. [30] is evaluated for $G=0$, $G'=0$ ground states, an $H=1$ excited state, and the linearly polarized incident fields of our model 3-level atom-field system. The resultant equation is transformed into the Wigner representation using

$$\rho(z,\bar{p}) = \frac{1}{2\pi\hbar}\int_{-\infty}^{\infty} dq\ \rho(\bar{p}+q/2,\bar{p}-q/2)e^{iqz/\hbar},$$

and one finds that ground state density matrix elements (in the "normal" representation) obey the following equation of motion:

$$\begin{aligned}\left(\frac{\partial}{\partial t}+i\omega_{aa_1}\right)\rho(a,a_1;z,p)+\frac{p}{M}\frac{\partial}{\partial z}\rho(a,a_1;z,p)\\ =-e^{-i\Omega_{jj'}t}e^{ik_{jj'}z}\left\{\frac{\chi^2 g(j,a_1)g(j',a_3)}{\gamma+i\Delta}\delta_{a_2a}\rho\left(a_2,a_3;z,p+\frac{1}{2}\hbar k_{jj'}\right)+\frac{\chi^2 g(j,a_2)g(j',a)}{\gamma-i\Delta}\delta_{a_3a_1}\rho\left(a_2,a_3;z,p-\frac{1}{2}\hbar k_{jj'}\right)\right\}\\ +\frac{1}{2}\chi^2 g(j,a_2)g(j',a_3)\left(\frac{1}{2}\delta_{\bar{K}0}+\frac{1}{4}\delta_{\bar{K}2}\right)\frac{\Gamma}{\gamma^2+\Delta^2}\delta_{a,a_1}e^{-i\Omega_{jj'}t}e^{ik_{jj'}z}\int_{-1}^{1}dx P_{\bar{K}}(z)\rho_0^0\left[a_2,a_3,z,p+\hbar\left(kz-\frac{k_j+k_{j'}}{2}\right)\right],\end{aligned}\quad\text{(A1)}$$

where a,a_1,a_2,a_3 label the two lower states and can equal 1 or 2, $P_{\bar{K}}(x)$ is a Legendre polynomial, $\gamma=\Gamma/2$, and $\omega_{aa_1}=(E_a-E_{a_1})/\hbar$. Several points should be made concerning this equation. First, there is a summation convention implicit in which repeated indices appearing on the right-hand side of the equation are summed over if they do not appear on the left hand side. Second, the sum over j and j' is from 1 to 4, corresponding to the four incident fields. Third, the Rabi frequencies associated with all the fields are taken to be equal, as is the branching ratio for each decay channel. Fourth, the

detunings of all the fields have been set equal when they appear in energy denominators associated with electronic state transitions, based on the assumption that $|\Omega_3-\Omega_1|$, $|\Omega_4-\Omega_2| \ll |\Delta|$. Fifth, the Kronecker delta δ_{a,a_1} reflects the neglect of any ground state coherence resulting from spontaneous emission. Finally, the g functions are defined by

$$g(j,1) = \delta_{j1} + \delta_{j3}, \quad g(j,2) = \delta_{j2} + \delta_{j4},$$

reflecting the fact that fields 1 and 3 drive only the 1-3 transition and fields 2 and 4 drive only the 2-3 transition.

To obtain a Fokker-Planck equation, one expands density matrix elements to second order in $\hbar$. When this is done, one finds

$$\left(\frac{\partial}{\partial t} + \frac{p}{M}\frac{\partial}{\partial z}\right)\rho_{12} = -(2\Gamma' + i\delta)\rho_{12} - 2i\Gamma'\sigma\left\{\cos(x)[\rho_{22}-\rho_{11}] - i\hbar k\sin(x)\frac{\partial}{\partial p}[\rho_{22}+\rho_{11}] + \hbar^2k^2\frac{\cos(x)}{2}\frac{\partial^2}{\partial p^2}[\rho_{22}-\rho_{11}]\right\}$$
$$-\Gamma'\left\{\cos(x)[\rho_{22}+\rho_{11}] - i\hbar k\sin(x)\frac{\partial}{\partial p}[\rho_{22}-\rho_{11}] + \hbar^2k^2\frac{\cos(x)}{2}\frac{\partial^2}{\partial p^2}[\rho_{22}+\rho_{11}]\right\}, \tag{A2}$$

$$\left(\frac{\partial}{\partial t} + \frac{p}{M}\frac{\partial}{\partial z}\right)\rho_{11} = -2\Gamma'\rho_{11} + 2i\Gamma'\sigma\left\{\cos(x)[\rho_{12}-\rho_{21}] + i\hbar k\sin(x)\frac{\partial}{\partial p}[\rho_{12}+\rho_{21}] + \frac{\cos(x)}{2}\hbar^2k^2\frac{\partial^2}{\partial p^2}[\rho_{12}-\rho_{21}]\right\} + \Gamma'[\rho_{11}+\rho_{22}]$$
$$+\frac{7}{10}\hbar^2k^2\Gamma'\frac{\partial^2}{\partial p^2}[\rho_{11}+\rho_{22}] - \frac{3}{10}\hbar^2k^2\Gamma'\cos(x)\frac{\partial^2}{\partial p^2}[\rho_{12}+\rho_{21}] - i\hbar k\Gamma'\sin(x)\frac{\partial}{\partial p}[\rho_{12}-\rho_{21}], \tag{A3}$$

where $x=2kz$, and a field interaction representation has been introduced [e.g., $\rho(1,2;z,p)=\rho_{12}(z,p)e^{i(\delta+\omega_{21})t}$; $\rho(a,a;z,p)=\rho_{aa}(z,p)$]. Equations for ρ_{21} and ρ_{22} are obtained by interchanging 1 and 2.

Defining

$$S = \rho_{22} + \rho_{11}, \tag{A4}$$

$$w = \rho_{22} - \rho_{11}, \tag{A5}$$

one can rewrite these equations as

$$\left(\frac{\partial}{\partial t} + \frac{p}{M}\frac{\partial}{\partial z}\right)S = \frac{7}{5}\hbar^2k^2\Gamma'\frac{\partial^2}{\partial p^2}S - 4\Gamma'\sigma\hbar k\sin(x)\frac{\partial}{\partial p}[\rho_{12}+\rho_{21}]$$
$$-\frac{3}{5}\hbar^2k^2\Gamma'\cos(x)\frac{\partial^2}{\partial p^2}[\rho_{12}+\rho_{21}], \tag{A6a}$$

$$\left(\frac{\partial}{\partial t} + \frac{p}{M}\frac{\partial}{\partial z}\right)w = -2\Gamma'w - 4i\Gamma'\sigma\left\{\cos(x)[\rho_{12}-\rho_{21}] + \hbar^2k^2\frac{\cos(x)}{2}\frac{\partial^2}{\partial p^2}[\rho_{12}-\rho_{21}]\right\}$$
$$-2i\hbar k\Gamma'\sin(x)\frac{\partial}{\partial p}[\rho_{12}-\rho_{21}], \tag{A6b}$$

$$\left(\frac{\partial}{\partial t} + \frac{p}{M}\frac{\partial}{\partial z}\right)\rho_{12} = -(2\Gamma' + i\delta)\rho_{12} - 2i\Gamma'\sigma\left\{\cos(x)w - i\hbar k\sin(x)\frac{\partial S}{\partial p} + \hbar^2k^2\frac{\cos(x)}{2}\frac{\partial^2 w}{\partial p^2}\right\}$$
$$-\Gamma'\left\{\cos(x)S - i\hbar k\sin(x)\frac{\partial w}{\partial p} + \hbar^2k^2\frac{\cos(x)}{2}\frac{\partial^2 S}{\partial p^2}\right\}. \tag{A6c}$$

The semiclassical description is valid only for $p \gg \hbar k$, energies greater than the recoil energy, and negligible spatial modulation of the total atomic density S [21,22]. In this limit, the only derivative on the right-hand side of Eqs. (A6b) and (A6c) that need be retained is $\partial S/\partial p$ and the spatial derivative of S can be dropped in Eq. (A6a). In this manner one arrives at Eqs. (5a) and (5b) of the text.

APPENDIX B

In this appendix, we provide the mathematical justification for the qualitative discussion of the origin of the friction force given in Sec. II.

1. Single pair of Raman fields

We consider first the friction force for a single pair of Raman fields, E_1 and E_2. To help elucidate the origin of the friction force, it proves useful to write down the density matrix equations for the full three-level system before adiabatic elimination of the ground-excited state coherence and the excited state populations. These equations, written in an interaction representation in which $\rho_{13}^{normal}=\tilde{\rho}_{13}e^{-i(kz-\Omega_1 t)}$, $\rho_{23}^{normal}=\tilde{\rho}_{23}e^{-i(-kz-\Omega_2 t)}$, and $\rho_{12}^{normal}=\tilde{\rho}_{12}e^{-i[2kz-(\Omega_1-\Omega_2)t]}$, and with the same approximations as in the text, are

$$\partial\rho_{11}/\partial t = i\chi_1(\tilde{\rho}_{13}-\tilde{\rho}_{31}) + \gamma_{3,1}\rho_{33}, \tag{B1a}$$

$$\partial\rho_{22}/\partial t = i\chi_2(\tilde{\rho}_{23}-\tilde{\rho}_{32}) + \gamma_{3,2}\rho_{33}, \tag{B1b}$$

$$\partial\rho_{33}/\partial t = -i\chi_1(\tilde{\rho}_{13}-\tilde{\rho}_{31}) - i\chi_2(\tilde{\rho}_{23}-\tilde{\rho}_{32}) - \Gamma\rho_{33}, \tag{B1c}$$

$$\partial\tilde{\rho}_{12}/\partial t = i\chi_2\tilde{\rho}_{13} - i\chi_1\tilde{\rho}_{32} - i\tilde{\delta}\tilde{\rho}_{12}, \tag{B1d}$$

$$\partial\tilde{\rho}_{13}/\partial t = i\chi_2\tilde{\rho}_{12} - i\chi_1(\rho_{33} - \rho_{11}) - (\gamma + i\Delta)\tilde{\rho}_{13}, \tag{B1e}$$

$$\partial\tilde{\rho}_{23}/\partial t = i\chi_1\tilde{\rho}_{21} - i\chi_2(\rho_{33} - \rho_{22}) - (\gamma + i\Delta)\tilde{\rho}_{23}, \tag{B1f}$$

$$\rho_{ji} = \rho_{ij}^*, \tag{B1g}$$

where $\gamma_{3,j}$ is the spontaneous decay from level 3 to level j ($\Gamma = \gamma_{3,1} + \gamma_{3,2}$) and $\tilde{\delta} = \delta - 2kv$. We have not yet imposed the assumptions of equal Rabi frequencies and equal branching ratios.

For the applied field

$$\mathbf{E}(z,t) = \frac{1}{2}\hat{\mathbf{x}}[E_1 e^{i(kz-\Omega_1 t)} + E_2 e^{i(-kz-\Omega_2 t)}] + \text{c.c.},$$

the friction force can be calculated using $F = \mathrm{Tr}[\rho\nabla(\mu\cdot\mathbf{E})]$, and one finds the spatially and temporally averaged friction force to be

$$\bar{F} = -\hbar\mathbf{k}[i\chi_1(\tilde{\rho}_{13} - \tilde{\rho}_{31}) - i\chi_2(\tilde{\rho}_{23} - \tilde{\rho}_{32})]. \tag{B2}$$

It then follows from Eqs. (B1a) and (B1b) that

$$\bar{F} = \hbar\mathbf{k}[(\gamma_{3,1} - \gamma_{3,2})\rho_{33} + \partial(\rho_{22} - \rho_{11})/\partial t]. \tag{B3}$$

In steady state, the averaged friction force vanishes regardless of the detuning $\tilde{\delta}$ and regardless of the ratio of the Rabi frequencies associated with the coupled transitions provided that the branching ratios of the two transitions are equal [15]. Even if the branching ratios are unequal, the steady-state, averaged friction force vanishes provided that $\tilde{\delta}=0$, since there is a dark state in this limit and $\rho_{33}=0$. Equation (B3) can be given a simple physical interpretation. In steady state, the second term vanishes and the force arises solely from scattered radiation. Each photon scattered on the 3-1 transition involves a loss of one photon from field E_1 and each photon scattered on the 3-2 transition involves a loss of one photon from field E_2, with a corresponding force on the atoms that is proportional to the scattering rates $\gamma_{3,1}$ and $\gamma_{3,2}$, respectively. If one is not in steady state, a time rate of change of the population difference of the ground states corresponds to a stimulated exchange of momentum between the fields resulting in a corresponding change in momentum of the atoms.

To make connection with the comments in Sec. II, we adiabatically eliminate $\tilde{\rho}_{13}$, $\tilde{\rho}_{31}$, $\tilde{\rho}_{23}$, $\tilde{\rho}_{32}$, and ρ_{33} from Eqs. (B1a)–(B1g), and revert to the approximations of equal Rabi frequencies and equal branching ratios to obtain the evolution equations

$$\frac{\partial w}{\partial t} = -\Gamma' w + 2i\sigma\Gamma'(\tilde{\rho}_{21} - \tilde{\rho}_{12}), \tag{B4a}$$

$$\frac{\partial\tilde{\rho}_{12}}{\partial t} = -(\Gamma' + i\tilde{\delta})\rho_{12} - i\sigma w - \frac{\Gamma'}{2}, \tag{B4b}$$

where $w=(\rho_{22}-\rho_{11})$ and $\sigma=\Delta/\Gamma$. With the same adiabatic elimination, Eq. (B3) for the friction force becomes

$$\bar{F} = -\hbar\mathbf{k}\Gamma'[w - 2i\sigma(\tilde{\rho}_{21} - \tilde{\rho}_{12})] = \hbar\mathbf{k}\partial w/\partial t,$$

the last equality following from Eq. (B4a). In steady state, the averaged friction force vanishes, resulting from a cancellation of the term proportional to the population difference w with that proportional to the ground state coherences $(\tilde{\rho}_{21} - \tilde{\rho}_{12})$. Each of these terms separately is nonvanishing if $\tilde{\delta} \neq 0$; i.e.,

$$w = \frac{2\tilde{\delta}\Gamma'\sigma}{\tilde{\delta}^2 + \Gamma'^2(1 + 4\sigma^2)}.$$

2. Two pairs of Raman fields

When two pairs of Raman fields are present, such as those shown in Fig. 1, it is no longer possible to eliminate the spatial dependence in all density matrix elements using a simple change of representation. Within the approximations of the main text, the appropriate equations for ground state density matrix elements and the friction force in terms of those elements can be derived using the equations of Ref. [17]. The density matrix equations are given in Eqs. (2), while the spatially and temporally averaged friction force is given by

$$\bar{F} = \hbar\mathbf{k}(\Gamma' + i\Delta)^{-1}\left\langle \begin{array}{c} (\chi_1^2 - \chi_3^2)\rho_{11} - (\chi_2^2 - \chi_4^2)\rho_{22} \\ +(\chi_1\chi_2 e^{2ikz} - \chi_3\chi_4 e^{-2ikz})\rho_{12} - (\chi_1\chi_2 e^{-2ikz} - \chi_3\chi_4 e^{2ikz})\rho_{21} \end{array} \right\rangle + \text{c.c.}, \tag{B5}$$

where $\langle\cdots\rangle$ represents a spatial average. The Rabi frequencies have not yet been set equal so that cancellations can be seen. It can be deduced immediately from Eq. (B5) that only the spatially homogeneous part of the ground state populations contribute to the averaged friction force. There are no contributions from spatially modulated components of the popu-lations (as occurs in Sisyphus cooling) since we have neglected interference between fields E_1 and E_3 (or E_2 and E_4) in driving *single* photon transitions. On the other hand, the components of the coherences ρ_{12} and ρ_{21} that are spatially modulated as $e^{\pm 2ikz}$ contribute to the averaged friction force.

For equal Rabi frequencies, the terms involving populations in Eq. (B5) cancel, reflecting the fact that changes in momentum arising from scattering from fields 1 and 3 (or 2 and 4) into vacuum field modes cancel one another. On the other hand, owing to different spatial phases associated with two-photon amplitudes proportional to E_1E_2 and E_3E_4, there is no cancellation of the terms involving the ground state coherences, except when $kz=n\pi$ (n is an integer). For equal Rabi frequencies, Eq. (B5) reduces to

$$\bar{F} = 4\hbar\mathbf{k}\Gamma'\sigma\langle\sin(2kz)(\rho_{12}+\rho_{21})\rangle. \tag{B6}$$

In general, owing to interference on two-photon transitions involving contributions with different spatial phases, there will be a nonvanishing contribution to the averaged friction force. Note that, for stationary atoms and zero detuning, $\rho_{12}=-\cos(2kz)/2$ and $\bar{F}=0$.

[1] J. Dalibard and C. Cohen-Tannoudji, J. Opt. Soc. Am. B **6**, 2023 (1989).

[2] P. J. Ungar, D. S. Weiss, E. Riis, and S. Chu, J. Opt. Soc. Am. B **6**, 2046 (1989).

[3] G. Nienhuis, P. van der Straten, and S.-Q. Shang, Phys. Rev. A **44**, 462 (1991).

[4] See, for example, S. Chang, B. M. Garraway, and V. G. Minogin, Opt. Commun. **77**, 19 (1990); P. R. Hemmer, M. G. Prentiss, M. S. Shahriar, and N. P. Bigelow, *ibid.* **89**, 335 (1992); R. Gupta, C. Xie, S. Padua, H. Batelaan, and H. Metcalf, Phys. Rev. Lett. **71**, 3087 (1993).

[5] B. Dubetsky and P. R. Berman, Laser Phys. **12**, 1161 (2002).

[6] M. Weitz, G. Cennini, G. Ritt, and C. Geckeler, Phys. Rev. A **70**, 043414 (2004).

[7] This condition is necessary to neglect the effects of fields E_1 acting on the 2-3 transition and E_2 acting on the 1-3 transition with regards to light shifts and optical pumping; however, it is possible to neglect the effect of fields E_2 and E_1 driving coherent transitions between levels 1 and 2 (with E_2 acting on the 1-3 transition and E_1 acting on the 2-3 transition) under the much weaker condition that the optical pumping rates be much smaller than ω_{21}.

[8] The condition needed to neglect modulated Stark shifts resulting from the combined action of fields E_1 and E_3 (or E_2 and E_4), as well as transitions between levels 1 and 2 resulting from fields E_1 and E_4 (or E_3 and E_2) is $|\Omega_3-\Omega_1|\gg|\chi\chi'/\Delta|$ and $|\Omega_4-\Omega_2|\gg|\chi\chi'/\Delta|$, where χ is a Rabi frequency associated with the 1-3 transition and χ' is a Rabi frequency associated with the 2-3 transition.

[9] B. Dubetsky and P. R. Berman, Phys. Rev. A **66**, 045402 (2002).

[10] J. Dalibard, Y. Castin, and K. Mølmer, Phys. Rev. Lett. **68**, 580 (1992); P. Marte, R. Dum, R. Taieb, and P. Zoller, Phys. Rev. A **47**, 1378 (1993).

[11] R. Zhang, N. V. Morrow, P. Berman, and G. Raithel (unpublished).

[12] P. R. Berman, V. Finkelstein, and J. Guo, in *Laser Spectroscopy X*, edited by M. Ducloy, E. Giacobino, and G. Camy (World Scientific, Singapore, 1992), pp. 15–20.

[13] C. Cohen-Tannoudji, in *Proceedings of the International School of Physics "Enrico Fermi," Course CXVIII*, edited by E. Arimondo, W. D. Phillips, and F. Strumia (North-Holland, Amsterdam, 1992), pp. 99–169.

[14] M. G. Prentiss, N. P. Bigelow, M. S. Shahriar, and P. R. Hemmer, Opt. Lett. **16**, 1695 (1991).

[15] F. Papoff, F. Mauri, and E. Arimondo, J. Opt. Soc. Am. B **9**, 321 (1992).

[16] Essentially the same equations result if one considers transitions between the $m=-1$ (state $|1\rangle$) and $m=1$ (state $|2\rangle$) sublevels of a $J=1$ ground state manifold of an atom in a magnetic field. In this case, one takes fields E_1 and E_3 to be polarized σ_+ and fields E_2 and E_4 to be polarized σ_-.

[17] P. R. Berman, G. Rogers, and B. Dubetsky, Phys. Rev. A **48**, 1506 (1993).

[18] The detunings of all the fields have been set equal when they appear in energy denominators associated with electronic state transitions, based on the assumption that $|\Omega_3-\Omega_1|$, $|\Omega_4-\Omega_2| \ll|\Delta|$.

[19] The interaction representation is one in which $\rho_{12}^{normal} =\rho_{12}e^{i(\Omega_1-\Omega_2)t}=\rho_{12}e^{i(\Omega_3-\Omega_4)t}$, where ρ_{12} is the density matrix element in the field interaction representation.

[20] Before adiabatic elimination of state $|3\rangle$, the contribution of spontaneous emission to the density matrix evolution is $\dot{\rho}_{11} =\dot{\rho}_{22}=(\Gamma/2)\rho_{33}$, $\dot{\rho}_{13}=-(\Gamma/2)\rho_{13}$, $\dot{\rho}_{23}=-(\Gamma/2)\rho_{23}$, and $\dot{\rho}_{33}= -\Gamma\rho_{33}$. After adiabatic elimination of state $|3\rangle$, the contribution of spontaneous emission to the density matrix evolution is $\dot{\rho}_{11}=-\Gamma'(\rho_{11}-\rho_{22})$; $\dot{\rho}_{22}=-\Gamma'(\rho_{22}-\rho_{11})$; $\dot{\rho}_{12}=-2\Gamma'\rho_{12}$, where Γ' is defined by Eq. (4e).

[21] Y. Castin, J. Dalibard, and C. Cohen-Tannoudji, in *Light Induced Kinetic Effects of Atoms and Molecules*, edited by L. Moi, S. Gozzini, C. Gabbanini, E. Arimondo, and F. Strumia (ETS Editrice, Pisa, 1990).

[22] V. Finkelstein, P. R. Berman, and J. Guo, Phys. Rev. A **45**, 1829 (1992).

[23] See, e.g., S. K. Dutta, B. K. Teo, and G. Raithel, Phys. Rev. Lett. **83**, 1934 (1999); N. V. Morrow and G. Raithel, Phys. Rev. A **70**, 051601(R) (2004).

[24] In the QMCWF, the creation of coherence via spontaneous emission is avoided by simulating a detection process that distinguishes between spontaneous emission into levels 1 and 2.

[25] R. Kosloff, J. Chem. Phys. **92**, 2087 (1988); C. Leforestier *et al.*, J. Comput. Phys. **94**, 59 (1991).

[26] S. Marksteiner, K. Ellinger, and P. Zoller, Phys. Rev. A **53**, 3409 (1996); H. Katori, S. Schlipf, and H. Walther, Phys. Rev. Lett. **79**, 2221 (1997).

[27] G. Raithel, G. Birkl, A. Kastberg, W. D. Phillips, and S. L. Rolston, Phys. Rev. Lett. **78**, 630 (1997).

[28] P. R. Berman, B. Dubetsky, and J. L. Cohen, Phys. Rev. A **58**, 4801 (1998).

[29] F. S. Cataliotti, R. Scheunemann, T. W. Hänsch, and M. Weitz, Phys. Rev. Lett. **87**, 113601 (2001). For applications to reduced period optical lattices, the copropagating fields used by these authors must be replaced by counterpropagating fields.

[30] B. Dubetsky and P. R. Berman, Phys. Rev. A **53**, 390 (1996).